Citric acid effect on the abundance, size and composition of water-dispersible soil colloids and its relationship to soil phosphorus desorption: a case study

Daniel Menezes-Blackburn[1*]; Roland Bol[2]; Erwin Klumpp[2]; Anna Missong[2]; Volker Nischwitz[2], Philip M. Haygarth[3]

1 Department of Soils, Water and Agricultural Engineering, CAMS, Sultan Qaboos University, PO Box 34, Al-khod 123, Sultanate of Oman

2. Forschungszentrum Jülich, Wilhelm-Johnen-Straße, 52428 Jülich, Germany

3 Lancaster University: Lancaster Environment Centre, Lancaster, LA1 4YQ, UK.

* danielblac@squ.edu.om

Abstract

Purpose: Citric acid exudation by plant roots is often linked to the mobilisation of recalcitrant soil phosphorus (P) for plant nutrition. In this case study, we have explored the effect of citric acid on the abundance, size and composition of water-dispersible soil colloids (WDC) to understand the mineral source of desorbed P and the chemical nature P-carrying mobilized colloids.

Methods: After incubation with citric acid, WDC were isolated using a soil particle-size fractionation method consisting of sedimentation, centrifugation and syringe filtration. The size range and composition of WDC was assessed using Field Flow Fractionation (FFF), combined with inductively coupled plasma mass spectrometry (ICP-MS) and UV spectrometry, for *in-vitro* P desorption assay samples under the influence of increasing doses of citric acid.

Results: Three sharp and well-defined FFF particle size fractions of WDC containing P (12-23, 23-36 and 36-300 nm), with elution times matching carbon (C) peaks and offset from Fe,

Al, and Si fractions. The concentration of soluble or WDC-associated P, C, Fe, Al and Si or increased in response to increasing citric acid doses. Silica colloids were only detected using syringe filtration below 5 µm. The Si, Fe and Al fine colloid fractions (<600nm) were positively correlated with P (de)sorption parameters measured by Diffusive Gradient in Thin films in previous work.

Conclusions: The P desorbed by citric acid originated predominantly from the disaggregation of Fe and Al oxides and silicate clays. The citric acid effect on mobilizing organic P carrying WDC fractions may increase soil organic P cycling and availability to plants.

Keywords: Soil colloids; Phosphorus availability; Phosphorus desorption; Citric Acid; Field Flow Fractionation;

1. Introduction

Among plant macronutrients, phosphorus (P) is perhaps the one with most limited bioavailability in soils due to its strong adsorption on soil particles and colloids, precipitation into insoluble forms and fixation into organic molecules (Vance et al. 2003). In order to maintain soil plant growth, P fertilisers are widely applied to cultivated soils, often in excess of plant net uptake (Syers et al. 2008). In many soils, this excessive P fertiliser use has led to a build-up of a large pool of “legacy” soil P and represents a high risk for nutrient pollution of waters, through runoff-associated P losses, which are directly linked with the eutrophication of receiving waters (Bol et al. 2018; George et al. 2018; Menezes-Blackburn et al. 2018).

The root exudation of low-molecular-weight organic acids is widely reported as an important plant-evolved mechanism for increasing soil P availability to plants (Almeida et al. 2018b; Hinsinger 2001; Jones 1998; Richardson et al. 2009). A strong scientific interest has been recently placed in the selection and genetic engineering of plants that exude organic acids into the rhizosphere (root-soil-interface) as a means to enhance P uptake and plant yields

(Lopez-Bucio et al. 2000; Tovkach et al. 2013). However, some cases have shown little success of this trait expression *in planta* (Ryan et al. 2014). Among the organic acids, citric acid is reported to be one of the most commonly naturally occurring root and microbial exudates reported to affect rhizosphere P availability (Clarholm et al. 2015; Rosas et al. 2008). Citric acid has been shown to induce higher P mobilisation than other organic acids (Gerke et al. 2000; Giles et al. 2012). The P mobilization mechanism is presumed to be related to the ability of organic acids to complex metal cations (Barrow et al. 2018), as well as competitive adsorption (Jones 1998; Wang et al. 2015). Citric and oxalic acid can also destabilize organic matter in the soil and facilitate the cycling of organically bound soil P (Clarholm et al. 2015). Citrate is expected to be, among common root exuded organic acids, the most effective in promoting P release through the chelation of aluminium (Al) in acidic soils, whereas oxalate tends to be more efficient in less acidic or calcareous soils (Clarholm et al. 2015). Little is known about how these organic acids affect P desorption and the disaggregation of P containing colloids.

We have explored in previous work the use of DGTs (diffusive gradient in thin films) to understand the dynamic resupply of P to soil solution in response to disturbances in the adsorption equilibrium caused by organic acids addition (Menezes-Blackburn et al. 2016a). Nevertheless, DGT studies do not offer any insights on the chemical nature of adsorbed/occluded P (Konrad et al. 2021), or the type and size of colloids (particles 1-1000 nm) that the labile P (desorbable) is associated with. In this study, we have for the first time explored this knowledge gap using Field Flow Fractionation (FFF) in combination with inductively coupled plasma mass spectrometry (ICP-MS) (Gimbert et al. 2003; Gottselig et al. 2017; Nischwitz et al. 2016) to address these research questions, widening the understanding of the mechanistic behaviour of this commonly reported root trait. Part of the P release induced by organic acids comes from the direct competition for adsorption sites and the dissolution of precipitated P caused by metal chelation (Menezes-Blackburn et al. 2018; Menezes-Blackburn et al. 2016a). Nevertheless, not all P desorbed is necessarily

originated from the same P pool. It is possible that some of this inorganic phosphate released into soil solution was hitherto unavailable for desorption, occluded in soil aggregates. We hypothesised that the dispersion of colloids by organic acids exposes these occluded P and allows for further P desorption. Namely, the appearance of different water-dispersible colloids (WDC) after the root exudation or addition of organic acids, concomitant with the increase in P desorption, provides evidence of the chemical nature of colloids, to which the newly released P was previously associated.

The aim of this *in vitro* study was to develop an in-depth understanding of P desorption relationship with soil colloid disaggregation by citric acid, a common plant root exudate. The specific objectives of this study were to quantify the effect of increasing dose of citric acid on: i) the concentration of P in WDC; ii) the contribution and role of amorphous and crystalline Si, Fe and Al colloids to soil P mobility and bioavailability; iii) the disaggregation of soil organic matter colloids containing phosphorus.

List of abbreviations

P_i - Inorganic phosphorus

P_o - Organic phosphorus measured as the difference between total and inorganic P

DGT - Diffusive gradients in thin films using a ferrihydrite containing gel as a P binding layer

DET - Diffusive equilibration in thin films (same DGT setup without the binding layer)

DIFS - ‘DGT Induced Fluxes in Soils and sediments’ model

P_{DET} (mg l^{-1}) - Pore water (dissolved) P concentration determined using DET

P_{DGT} (mg l^{-1}) - DGT measured time averaged soil solution P concentration at the surface of DGT device

P_E - Effective P concentration – DGT estimated soil solution P + labile P concentration from the solid phase.

P_{Olsen} (mg kg^{-1}) - Phosphorus concentration (solid phase) measured using $NaHCO_3$ extraction

D_0 (cm^2 s^{-1}) - Diffusion coefficient in diffusive layer of DGT device

D_s (cm^2 s^{-1}) - Diffusion coefficient in soil

k_{-1} (s^{-1}) - Desorption rate constant

k_1 (s^{-1}) - Sorption rate constant

K_{dl} (cm^3 g^{-1}) - Equilibrium distribution coefficient between solid phase and soil solution

R - Ratio of P_{DGT} to P_{DET}

R_{diff} - Ratio of P_{DGT} to P_E in the case where there is no P resupply from the solid phase, estimated using DIFS for diffusion only case

T_c (s) - Response time of (de)sorption process

WDC - water-dispersible colloids

FFF - Field Flow Fractionation of WDC by particle size

ICP-MS - Inductively coupled plasma mass spectrometry analysis of the elemental composition of WDC eluted from the FFF

2. Material and methods

2.1 Soil sample and previous data

The sample used in this study is a topsoil (0-10 cm depth) from the Glensaugh Research Station in Laurencekirk, Aberdeenshire (Glensaugh soil, 56º53'42.29"N -2º32'00.42"W), in Scotland, UK. The Glensaugh soil is a freely drained Podzol (FAO 1994). The same soil was used to understand the effect of root exudates on phosphorus desorption kinetics and bioavailability to plants using diffusive gradients in thin films techniques (Menezes-Blackburn et al. 2016a). The chosen sample was previously characterised for pH, oxalate extractable Al and Fe, soil organic carbon (C_{org}), microbial biomass P, total P and inorganic P in $NaHCO_3$ (Olsen), NaOH, citric acid and water-extractable P concentrations as (Table 1). Additionally, the effect of citric acid on the soil P desorption was evaluated by Menezes-Blackburn et al. (2016b) using diffusive gradient in thin films methods (DGT; Table S1). The findings from study are contranined to the soil type and charachteristics, and the methods here presented need to be applied in a more simplified way to a higher number of samples before extrapolations can be made across the landscape.

2.2 Sample processing and particle separations

In this study, the time-effect associated with the disaggregation of soil colloids containing P, Si, Fe, Al, and C was assessed after the citric acid addition (10 mM kg^{-1} soil). and the citric acid dose effect was evaluated 24 h after the start of the incubation. Altogether, the used soil citric acid incubation conditions were tested and established in a series of preliminary experiments to our previous manuscript on the effect citric acid on P desorption using the same soil (Menezes-Blackburn et al. 2016a). In short, for the incubation of soils with citric acid, samples (5 g DW) were adjusted to 50% of field capacity with MilliQ water two days before processing. Twenty-four hours before processing, the soil was prepared by adjusting soil moisture content to 80% of field capacity with a citric acid (CA) solution, with six doses used in quadruplicate incubations: 0, 2, 4, 6, 8 and 10 mmol kg^{-1} as described by Menezes-Blackburn et al. (2016a). Incubations of soils with citric acid at 10 mmol kg^{-1} applied at different times (0,1,12 and 24 h) were also performed in quadruplicate for obtaining insights on the kinetics of the soil disaggregation after addition of citric acid. Our incubation conditions represent an improvement with regards to many other studies on the effect of citric acid in soils, representing these natural systems in a more realistic manner. Namely, soils were incubated at field-like moisture content, and the citric acid dose was established in mg kg^{-1} of dry soil weight, unlike the usual incubations at high liquid-to-solid ratios and doses calculated in mg L^{-1} of suspension.

After incubation of soils with citric acid at field-like moisture conditions minimising interferences, WDC were isolated using a soil particle-size fractionation method consisting of: a) shaking and sedimentation step (1h at 100 rpm and soil-to-water mass ratio 1:8); b) centrifugation at 3000 g for 3 min; c) syringe filtration of aliquots of the supernatant at 0.22 µm and 5 µm. These separation conditions were well established and validated in previous studies to represent fine colloids labile for being leached and carried by runoff waters,

including those organic or containing adsorbed P (Gottselig et al. 2017; Jiang et al. 2017; Jiang et al. 2015a; Jiang et al. 2015b; Missong et al. 2016; Missong et al. 2018).

2.3 Field flow fractionation of soil colloids

We used an AF4 (asymmetric Flow Field Flow Fractionation) system (Postnova, Landsberg, Germany) with a 1 -kDa polyethersulfone (PES) membrane and 500-µm spacer for size-fractionation of the particles in suspension with ultrapure water (pH: 5.5, Milli-Q). The AF4 was coupled online to a UV detector (Postnova Analytics) for assessing UV spectra as proxies for organic matter, to a DLS detector for measuring the hydrodynamic diameters of particles, and to an ICP–MS system (Agilent 7500, Agilent Technologies) for monitoring the Fe, Al, silicon (Si), C, manganese (Mn) and P contents of the particles in the suspensions. A 25 µM NaCl solution at pH 5.5 served as the carrier. The injected sample volume was 1 mL, and the focusing time was 17 min, with 3 mL min^{-1} crossflow. The elution was performed by 8 min of constant 3 mL min^{-1} cross flow followed by 10 min linear decrease to 0 mL min^{-1} crossflow. During the focusing time, small particles with size <1 kDa including truly dissolved P species and dissolved other ions passed through the PES membrane, and only WDC-bound elements remained in the separation channel. The quantification strategy via post channel calibration was adopted from our previous work (Missong et al. 2018). Sulphate latex standard particles (Postnova Analytics) with hydrodynamic diameters of 20, 60, 100, 250 and 600 nm (nominal sizes) were analysed for the size calibration using the same AF4 method. The integrated peaks were expressed in mg kg^{-1} soil, and the ratios between them were also explored.

Statistical analyses

The citric acid treatments and incubation conditions were performed in quadruplicate as described in section 2.2, and the colloidal fractions abundance and composition were

assessed as described in section 2.3. The effect of citric acid in the different response parameters measured was evaluated by analysis of variance (one-way ANOVA), and means were separated using the Tukey test ($p < 0.05$). For every data set, the standard deviation was also determined and presented as error bars. Pearson correlation between the elemental concentration of different colloidal FFF peaks and P bioavailability and desorption kinetics parameters was used as an exploratory tool to evaluate these response variables' interdependency.

3. Results

3.1 Effect of citric acid on water dispersible soil colloids

Our data suggests that citric acid caused an overall increase in the abundance of smaller sized water-soluble Fe, Al, Si and C colloids. The analysis of the extracts filtered to below 5 µm tended to show a low signal to noise ratio and a less clear definition of peaks (Figure S1 and S2). Additionally, elution time of peaks was often not exactly coincident between the two filter extracts. These filtration treatments appear to exclude particles below the expected membrane cut off, likely due to the blockage of filter pores. The extracts filtered to below 5 µm contained the highest amount of Si-containing colloids (aluminosilicate clays). They were used to understand aluminosilicate disaggregation and possible association with P colloids appearance and P desorption kinetics. For the other investigated elements (P, Fe, Al and C), the FFF analysis with soil WDC filtered at 0.22 µm was, in general, considered more precise (Figures 1, 2 and 3). Nanoparticles (1-100 nm) in this study were over 1 kDa due to the chosen PES membrane used in FFF analysis. The size range for the colloidal particles analysed in this study are estimated to be from 1 nm to about 1000 nm.

Carbon and phosphorus-containing colloids of the 0.22 µm filtrates appeared in three peaks ranging from 12 to 23 nm (maximum at approximately 22 nm), 23 to 36 nm (maximum at approximately 25 nm) and 36 to 300 nm (maximum at approximately 55 nm), respectively

(figures 1A and 1B). The excellent matching of the elution times and shape of the peaks of P and C colloids, as well as the mismatch between P peaks and Fe, Al and Si peaks, suggests that the organic P species or inorganic phosphorus species associated to organic matrix are the predominant form of colloidal P in our study soil. These correspond up to half of the water-extractable total P, measured by ICP-MS after syringe filtered through 0.22 µm PES membrane. The chemical nature of these organic P species was not investigated in detail in this study and needs to be further studied. The broad shape of C peaks and the high C:P ratios found indicates that these organic P correspond to below 1% of the total organic colloids detected (Table S2).

Similar to C and P, Fe and Al-containing colloids also appeared in three defined offset peaks ranging from 12 to 23 nm (maximum at approximately 14 nm), 23 to 54 nm (maximum at approximately 36 nm) and 54 to >600 nm (maximum at approximately 265 nm), respectively (Figures 2A and 2B). Note, over 90% of these elements occurred in the first peak. The occurrence of the third peak indicates a possible reaggregation of these colloids, due to the presence of larger particles than expected to the 0.22 µm filtrate. The fact that the Fe and Al showed peaks at the same elution times suggests that they could be part of the same colloids associated with Fe-Al hydroxides. At the highest citric acid dose and incubation times, the first Fe and Al peak (12-23 nm) showed a small shoulder peak at 17 nm which is slightly more aligned with the P peak at 22 nm, and may indicate some presence of iron in P containing nanoparticles hidden beneath the bigger Al and Fe peaks. Nevertheless, this assessment is rather speculative. With the increase of citric acid dose the Al:Fe ratio was decreased from 1.1 to 0.6 (Table S2), thereby showing that Al concentration is lower when citric acid is present. The exact nature these colloids need to be further elucidated.

Silica nanoparticles were nearly absent in the filtrate <0.22 µm for most of the citric acid doses. In the 5 µm filtrate, colloids were abundantly found in two broad peaks of about 26 to 60 nm (maximum at approximately 31 nm), and 60 to >600 nm (maximum at approximately

270 nm), respectively (Figures 3A and 3B). Overall, these Fe, Al and Si-containing colloids were not associated with P due to different peak elution times in FFF fractograms.

3.2 Kinetics of citric acid effect on water-extractable soil colloids

The P concentration in colloids below 0.22 µm was not significantly changed between 0 and 24h, suggesting that at this scale, the effect of citric acid is near to immediate (minutes). Nevertheless, total P concentrations in these extracts are significantly reduced in time from 2.4 to 0.9 mg kg^{-1} soil between 0 and 24h (Table 2). The colloids containing P analysed in the filtrate < 5 µm showed a significant increase between 0 and 2h, with a slight decrease thereafter.

Iron and Al FFF fractograms showed similar behaviour, with a strong peak at the range of 16 to 18 nm when filtered through 0.22 µm (Figure 2A and 2B), and two additional peaks (26-37 nm and 37 to 1000 nm) when filtered through 5 µm (Figure S2). The kinetic behaviour of the elemental concentrations associated with colloids in the filtrates with different membrane cut off was remarkably different. For the extracts filtered through 0.22 µm, the amount of Fe and Al-containing colloids tends to increase in time 2h after the addition of citric acid, nearly tripling its initial concentration at 24h for the case of Fe (Figure 2C and 2D). Whilst for the <5 µm filtrate, the amount of Fe and Al-containing colloids tends to increase at 2 h of incubation, and decreasing afterwards (Figure S2C and S2D).

Silica colloids were significantly detected at 10 mmol kg^{-1} citric acid dose in the extracts filtered through 0.22 µm (Figure 3E). In this extract, the small amount of Si-containing colloids even tends to decrease in time during the 24h incubation (Figure 3C), suggesting that the effect of citric acid on the disaggregation of aluminosilicate clays is immediate and not lasting. In contrast to the other elements evaluated, the Si fractograms were much better developed in the extracts filtered through 5 µm (Figure 3B). For these extracts, two peaks of 26-38 and 38-600 nm were observed, the first much smaller than the second. These peaks showed contrasting kinetic behaviour: the 26-38 nm Si-containing nanoparticles tended to

increase during the 24 h incubation time whilst the 38-600 nm peak tended to decrease during the 24h incubation with citric acid (Figure 3D). Moreover, these Si peaks from the <5 µm filtrate are similarly placed with the Al and Fe peaks in the same filtrates (Figure S2). This is indicative of clay minerals with some structural Fe, embedded into the crystalline structure. Such Fe-bearing clay mineral colloids were recently reported by Jiang *et al.* (2015a) using similar methods to the ones here described.

3.3 Dose-response of citric acid effect on P associated with soil colloids

Concentrations of P associated to colloids oscillated between 180 µg kg^{-1} in the soil without citric acid addition to 400 µg kg^{-1} in the soils with 10 mM citric acid addition for WDC syringe filtered to below 0.22 µm (Figures 1C and 1E). Similarly, in the fractions filtered to below 5 µm, the citric acid addition increased the P concentration associated to colloids from 300 to 590 µg kg^{-1} (Figure S1). These values were considered high and corresponded to up to 50% of the total P concentrations in these water extracts.

Carbon, Fe and Al WDC increased in response to the addition of citric acid, nevertheless, P colloids appear to be predominantly associated with carbon-containing colloids. Silica colloids were nearly absent in the filtrate <0.22 µm and, in the 5 µm filtrate, they were abundantly found in two broad peaks not associated with P.

3.4 Pearson correlation between elemental concentration in nanoparticles and phosphorus desorption kinetic parameters

A Pearson's correlation table between the concentration of P, Fe, Al, Si and C in colloids against the P bioavailability parameters and parameters reflecting the P desorption kinetics was assembled in order to link P desorption to the original soil aggregates where desorbed P was previously occluded in (Table 2). The P desorption parameters (Table S1) are

reported by Menezes-Blackburn *et al.* (2016a) from which the experimental conditions were exactly reproduced in this study. Phosphorus and carbon-containing colloids of all sizes, were strongly positively correlated with P in soil solution (P_{DET}), DGT extractable P (P_{DGT}) and the effective P concentration (P_E) and negatively correlated with the P desorption parameters (Desorpt, R, R-$R_{diff,}$ Tc, K_1, K_{-1}), as expected, since P induced by citric acid addition induces a decrease in further desorption rate, both by affecting the gradient and the chemical nature of the P associated with the solid phase (Menezes-Blackburn et al. 2016a). Small Fe and Al-containing nanoparticles (14-26 nm) were also positively correlated with P concentration in soil solution whilst the larger fractions (>60 nm) were negatively correlated with the same parameter. Silica nanoparticles (14-60 nm) were poorly correlated with P in soil solution and P desorption kinetic parameters. Nevertheless, they were strongly correlated with Olsen P, commonly used as a P bioavailability indicator for crops.

4. Discussion

Three sharp well-defined particle size peaks were observed in FFF for P-containing colloids, and the smallest was below 20 nm, the second peak was about 30 nm and the third of about 60 nm. This size distribution is in agreement with studies in soil leachates and stream waters where P associated nanoparticle size fractions are usually reported in size ranges of 1 to 20 nm and 20 to 70 nm and are commonly termed "natural" nanoparticles (Gottselig et al. 2017; Missong et al. 2018). In our study, the appearance of these peaks was well aligned (elution time) with the C peaks and apparently not associated directly with Si. Aluminium and Fe-containing nanoparticles were strongly increased by the addition of citrate, the reaction was dose-dependent and continued developing in time during the 24h incubation, and may have continued thereafter. This is evidence that the exudation of organic acids is associated with the disaggregation of Fe and Al (hydr)oxides, common in acidic soils such as the one chosen for this study.

Two co-occurring phenomena are happening in response to citric acid addition to soils: i) the first is the disaggregation of micro-aggregates into its constituent fine colloids (Jiang et al. 2017; Krause et al. 2020; Missong et al. 2018), which appear in our fractograms as an increase in the nanoparticle peaks at increasing citric acid dose with a concomitant decrease in higher sized colloidal peaks (Jiang et al. 2015a); ii) The second is the desorption of P compounds and other elements from the surface of these colloids (Menezes-Blackburn et al. 2016a; Menezes-Blackburn et al. 2016b), indicated by the increase in soluble P in soil solution (measured by diffusive equilibration in thin films passive sampler; C_{DET}) at increasing citric acid doses. The molecular mechanisms behind the disaggregation of colloids by citric acid are related to the surface chemistry of each colloid and their interaction with citric acid molecules (Shinohara et al. 2018), as well as on the extent of polyvalent metal chelation, decreasing the flocculation and aggregate size of these colloids (Jiang et al. 2015a; Jiang et al. 2015b). It is generally expected that colloidal Fe and organic C regulates the stability of soil microaggregates (Krause et al. 2020). Citric acid is known to be able to dissolve surface Fe this is assumed to play a major role in inducing P desorption from acid soils (Barrow et al. 2018), here we suggest that it also plays a central role in colloidal disaggregation. This disaggregation exposes occluded P increasing P total desorption and, at the same time, the initial desorption of P induced by citric acid addition induces a decrease in the desorption rate constant (K_{-1}), both by affecting the solid-to-solution P concentration gradient and the chemical nature of the P associated with the solid phase (Menezes-Blackburn et al. 2016a). In our study, the appearance of colloids of different composition was used in the correlation analysis with P bioavailability and desorption kinetic data produced by Menezes-Blackburn et al. (2016a) using Diffusive Gradient in Thin films (DGT) and the same soil and incubation conditions of this study. A positive correlation between the soil solution P and the appearance of a given colloid fraction indicates that the P desorption may have occurred from P occluded in the soil aggregates that were dispersed by the addition of citric acid. This allowed to draw insights on which colloid size and type carries the adsorbed P that can be mobilised by the root exudation of citric acid. Based on

this analysis, for our studied soil, surprisingly the desorbed P appears to be originated predominantly from C, Al and Fe, rather than from Si containing colloids. Organic C is involved in the micro- or nano-aggregates stability as a cementing agent (Haygarth et al. 1997; Krause et al. 2020). In addition, Fe and Al colloids were highly correlated with P (de)sorption parameters, suggesting that most of the soluble P was originated from the disaggregation of Fe and Al (hydr)oxides. Since bigger Fe and Al size fractions detected (>60 nm) were negatively correlated with P bioavailability data, we hypothesise that these Fe- and Al-containing colloids may be metal bridged micro-aggregates (Clarholm et al. 2015), prone to be further dispersed by the addition of increasing citric acid doses, exposing occluded P (organic and inorganic) and allowing for its desorption.

Si-containing nanoparticles of low size (14-60 nm) were the only ones highly negatively correlated with Olsen P. Nevertheless, these are found in low amount and are barely over the detection limit. Bigger sized Si particles and microaggregates (60-1000k nm), which account for almost all the Si colloids, showed a low positive correlation with Olsen P and the solid to solution distribution ratio (K_{dl}), and negatively correlated with soil solution P (P_{DET}) and bioavailable P (P_{DGT}). This behaviour is the opposite of the observed from C, Fe and Al colloids, an indication that Si colloids may be related to Olsen P and not to soil solution and bioavailable P. Suggesting that bicarbonate extractable P (commonly used as P bioavailability indicator) is, for our soil, may be biased towards aluminosilicate associated P. Interestingly, Si colloids were positively correlated with P desorption parameters indicating the speed of P desorption is increased with the increase in these Si colloids, but not its overall lability. The DGT extractable P and effective P concentration calculated thereafter were shown in previous studies to be better predictors of plant P uptake than Olsen P for many different soils and ecosystems (Mason et al. 2010; Six et al. 2013). In our study, DGT parameters were better correlated with the appearance of Fe and Al in colloids after the addition of citric acid at different doses, which suggests that DGTs may be better predictors of P bioavailability in the situation where aluminosilicate clays are not the immediate source

of soil labile P that can be depleted by plants through the exudation of organic acids. These hypotheses should be tested in further studies for unveiling clearer evidence than the ones here presented.

Since citric acid increases the organic P species or inorganic P species associated to nanoparticulate organic matrix in water extracts (Wei et al. 2010), it appears to be dissociating P-SOM associates. Organic P is not immediately available to plants and needs to be hydrolysed before the plant uptake of its covalently bound phosphate moieties. Nevertheless, the fact that P containing colloids are appearing after the addition of a metal chelator such as citric acid, indicates the presence of supramolecular aggregates stabilised by the polyvalent metal cations bridging of SOM functional groups (Clarholm et al. 2015). Organic phosphorus enrichment in soil colloids was recently shown by 31P-NMR (Jiang et al. 2015b; Liu et al. 2014; Missong et al. 2016; Wang et al. 2020). Jiang *et al.* (2017) also reported the potential release of nano-sized organic matter-Fe/Al-P colloids affected by the stagnic properties along a grassland transect from Cambisol to Stagnosol. The destabilisation of this SOM aggregates and the release of nano-scale soil organic P may be a critical step that might facilitate its hydrolysis by allowing physical access of hydrolytic enzymes (phosphatases) to act on the now exposed phosphorus moieties, allowing its mineralisation and subsequent P plant uptake (Clarholm et al. 2015; Menezes-Blackburn et al. 2018; Menezes-Blackburn et al. 2013). In a field experiment using a high citric acid exuding ruzigrass (*Brachiaria ruziziensis*) in rotation with soybean (*Glycine max*) in a Brazilian Oxisol, the soil concentration of recalcitrant P was significantly reduced in comparison to fallow treatment (Almeida et al. 2018a), indicating that citric acid exudation can be linked to the *in vivo* cycling and scavenging for soil stabilised organic phosphorus.

5. Conclusions

For our studied soil, P nanoparticles mobilised by the citric acid addition appear to be mostly associated with organic matter as evidenced by the elution time of the peaks on the

fractograms obtained with a hyphenated field-flow fractionation with inductively coupled plasma mass spectrometry and a signal detector. At the same time, colloidal P was not associated directly with Fe, Al and Si. However, the appearance of Fe and Al in colloids at increasing doses of citric acid were correlated with diffusive gradient in thin films derived P (de)sorption and bioavailability parameters, suggesting that a significant amount of the mobilised P was originated from Fe and Al (hydr)oxides colloids, confirming our initial hypothesis. Silica nanoparticles of 26-60 nm were the only colloidal fraction positively correlated with Olsen P, suggesting that bicarbonate extractable P may be biased towards aluminosilicate associated P. Our case study provides new evidence for (i) the link between citric acid exudation and P desorption from Fe and Al-containing colloids, and (ii) the mobilisation of nanoparticulate organic matter-associated P. This desorbed organic P may subsequently become more prone to be hydrolysed by enzymes produced by the soil microbial community, and ultimately become available to plants.

Funding This work was performed with financial support of the Organic Phosphorus Utilisation in Soils (OPUS) project, funded by Biotechnology and Biological Sciences Research Council (BBSRC) responsive mode grant (BB/K018167/1) in the UK to explore cropping strategies to target the use of recalcitrant soil P_o. We thank the OPUS team for the important work leading to this manuscript, especially Prof. Hao Zhang, Dr. Courtney D. Giles, Dr. Tegan Darch, Dr. Marc Stutter, Dr. Timothy S. George, Dr. Charles Shand, Dr. David Lumsdon, Patricia Cooper, Renate Wendler, Dr. Lawrie Brown, Dr. Martin Blackwell and Dr. Catherine Wearing. The first author received financial support from Sultan Qaboos University through the projects RF/AGR/SWAE/18/01 and IG/AGR/SWAE/19/02, as well as the Alexander von Humboldt Foundation through a renewed research stay fellowship. The authors appreciate the additional in-kind support from SQU, Oman.

Compliance with Ethical Standards

Conflict of Interest The authors declare that they have no conflict of interest.

Bibliography:

Almeida DS, Menezes-Blackburn D, Turner BL, Wearing C, Haygarth PM, Rosolem CA (2018a) Urochloa ruziziensis cover crop increases the cycling of soil inositol phosphates Biol Fertil Soils 54:935-947

Almeida DS, Menezes-Blackburn D, Rocha KF, de Souza M, Zhang H, Haygarth P, Rosolem C (2018b) Can tropical grasses grown as cover crops improve soil phosphorus availability? Soil Use Manage 34:316-325

Barrow NJ, Debnath A, Sen A (2018) Mechanisms by which citric acid increases phosphate availability Plant Soil 423:193-204 doi:10.1007/s11104-017-3490-8

Bol R et al. (2018) Challenges of reducing phosphorus based water eutrophication in the agricultural landscapes of Northwest Europe Front Mar Sci 5:1-16

Clarholm M, Skyllberg U, Rosling A (2015) Organic acid induced release of nutrients from metal-stabilized soil organic matter -The unbutton model Soil Biol Biochem 84:168-176

George TS et al. (2018) Organic phosphorus in the terrestrial environment: a perspective on the state of the art and future priorities Plant Soil 427:191-208

Gerke J, Beißner L, Romer W (2000) The quantitative effect of chemical phosphate mobilization by carboxylate anions on P uptake by a single root. I. The basic concept and determination of soil parameters J Plant Nutr Soil Sci 163:207-212

Giles CD, Richardson AE, Druschel GK, Hill JE (2012) Organic Anion-Driven Solubilization of Precipitated and Sorbed Phytate Improves Hydrolysis by Phytases and Bioavailability to Nicotiana tabacum Soil Sci 177:591-598

Gimbert LJ, Andrew KN, Haygarth PM, Worsfold P (2003) Environmental applications of flow field-flow fractionation (FIFFF) Trends Anal Chem 22:615-633

Gottselig N et al. (2017) Phosphorus binding to nanoparticles and colloids in forest stream waters Vadose Zone J 16

Haygarth PM, Warwick MS, House WA (1997) Size distribution of colloidal molybdate reactive phosphorus in river waters and soil solution Water Res 31:439-448

Hinsinger P (2001) Bioavailability of soil inorganic P in the rhizosphere as affected by root-induced chemical changes: a review Plant soil 237:173-195

Jiang X et al. (2017) Colloid-bound and dissolved phosphorus species in topsoil water extracts along a grassland transect from Cambisol to Stagnosol Biogeosci 14:1153-1164

Jiang X et al. (2015a) Phosphorus containing water dispersible nanoparticles in arable soil J environ qual 44:1772-1781

Jiang X, Bol R, Willbold S, Vereecken H, Klumpp E (2015b) Speciation and distribution of P associated with Fe and Al oxides in aggregate-sized fraction of an arable soil Biogeosci 12:6443-6452

Jones DL (1998) Organic acids in the rhizosphere - a critical review Plant Soil 205:25-44

Konrad A, Billiy B, Regenbogen P, Bol R, Lang F, Klumpp E, Siemens J (2021) Forest Soil Colloids Enhance Delivery of Phosphorus Into a Diffusive Gradient in Thin Films (DGT) Sink Front For Global Change 3

Krause L, Klumpp E, Nofz I, Missong A, Amelung W, Siebers N (2020) Colloidal iron and organic carbon control soil aggregate formation and stability in arable Luvisols Geoderma 374:114421

Liu J, Yang J, Liang X, Zhao Y, Cade-Menun BJ, Hu Y (2014) Molecular speciation of phosphorus present in readily dispersible colloids from agricultural soils Soil Sci Soc Am J 78:47-53

Lopez-Bucio J, de la Vega OM, Guevara-Garcia A, Herrera-Estrella L (2000) Enhanced phosphorus uptake in transgenic tobacco plants that overproduce citrate Nature biotechnol 18:450-453

Mason S, McNeill A, McLaughlin MJ, Zhang H (2010) Prediction of wheat response to an application of phosphorus under field conditions using diffusive gradients in thin-films (DGT) and extraction methods Plant soil 337:243-258

Menezes-Blackburn D et al. (2018) Opportunities for mobilizing recalcitrant phosphorus from agricultural soils: a review Plant Soil 427:5-16

Menezes-Blackburn D, Jorquera MA, Greiner R, Gianfreda L, de la Luz Mora M (2013) Phytases and phytase-labile organic phosphorus in manures and soils Crit Rev Environ Sci Technol 43:916-954

Menezes-Blackburn D et al. (2016a) Organic Acids Regulation of Chemical–Microbial Phosphorus Transformations in Soils Environ sci technol 50:11521-11531

Menezes-Blackburn D et al. (2016b) A holistic approach to understanding the desorption of phosphorus in soils Environ sci technol 50:3371-3381

Missong A, Bol R, Willbold S, Siemens J, Klumpp E (2016) Phosphorus forms in forest soil colloids as revealed by liquid-state 31P-NMR J Plant Nutr Soil Sci 179:159-167

Missong A et al. (2018) Leaching of natural colloids from forest topsoils and their relevance for phosphorus mobility Sci Total Environ 634:305-315

Nischwitz V, Gottselig N, Missong A, Meyn T, Klumpp E (2016) Field flow fractionation online with ICP-MS as novel approach for the quantification of fine particulate carbon in stream water samples and soil extracts J Anal At Spectrom 31:1858-1868

Richardson AE, Hocking PJ, Simpson RJ, George TS (2009) Plant mechanisms to optimize access to soil phosphorus Crop Pasture Sci 60:124-143

Rosas A, Pinilla L, Menezes-Blackburn D, Mora ML (2008) Exudation of Organic Acids in Ryegrass and White Clover in Response to Different Phosphorous and Manganese Doses J Soil Sci Plant Nutr 8:233-234

Ryan PR et al. (2014) Can citrate efflux from roots improve phosphorus uptake by plants? Testing the hypothesis with near-isogenic lines of wheat Physiol plant 151:230-242

Shinohara S, Eom N, Teh E-J, Tamada K, Parsons D, Craig VS (2018) The Role of citric acid in the stabilization of nanoparticles and colloidal particles in the environment: measurement of surface forces between hafnium oxide surfaces in the presence of citric acid Langmuir 34:2595-2605

Six L, Smolders E, Merckx R (2013) The performance of DGT versus conventional soil phosphorus tests in tropical soils—maize and rice responses to P application Plant and Soil 366:49-66

Syers J, Johnston A, Curtin D (2008) Efficiency of soil and fertilizer phosphorus use. Reconciling changing concepts of soil phosphorus behaviour with agronomic information. FAO Fertilizer and Plant Nutrition Bulletin 18 Food and Agriculture Organization of the United Nations, Rome, Italy

Tovkach A et al. (2013) Transposon-mediated alteration of TaMATE1B expression in wheat confers constitutive citrate efflux from root apices Plant Physiol 161:880-892

Vance CP, Uhde-Stone C, Allan DL (2003) Phosphorus acquisition and use: critical adaptations by plants for securing a nonrenewable resource New Phytol 157:423-447

Wang L, Missong A, Amelung W, Willbold S, Prietzel J, Klumpp E (2020) Dissolved and colloidal phosphorus affect P cycling in calcareous forest soils Geoderma 375:114507

Wang Y, Chen X, Whalen JK, Cao Y, Quan Z, Lu C, Shi Y (2015) Kinetics of inorganic and organic phosphorus release influenced by low molecular weight organic acids in calcareous, neutral and acidic soils J Plant Nutr Soil Sci 178:555-566

Wei L, Chen C, Xu Z (2010) Citric acid enhances the mobilization of organic phosphorus in subtropical and tropical forest soils Biol Fert Soils 46:765-769

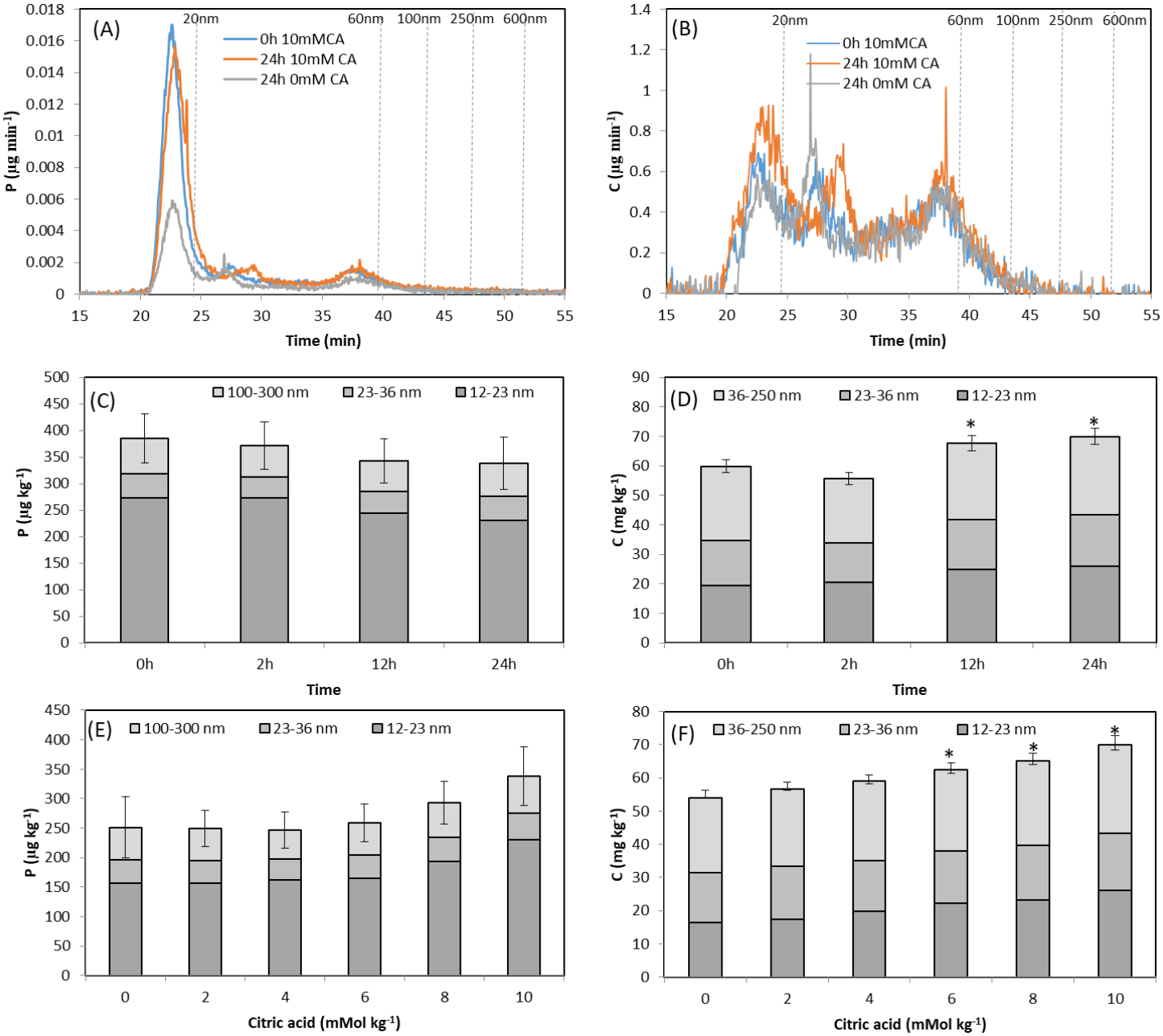

Figure 1. Phosphorus (A) and carbon (B) fractograms from asymmetric flow field-flow fractionation coupled to ICP-MS analysis of water dispersed soil colloids before and after incubation with citric acid at increasing doses (filtered through 0.22 µm). Vertical dash lines mark the elution time of latex standards peaks (20, 60, 100, 250 and 600 nm). Integration of fractogram peaks for increasing incubation time (0, 2, 12 and 24) and citric acid dose of 10 mMol kg^{-1} soil for phosphorus (C) or carbon (D). Integration of fractogram peaks for increasing citric acid dose (0, 2, 4, 6, 8, 10 mMol kg^{-1} soil) after 24 h of citric acid addition for phosphorus (E) or carbon (F). Error bars represent standard deviation and * denote significant difference with respect to their respective controls (0 time or 0 dose, $P<0.05$, Tukey test).

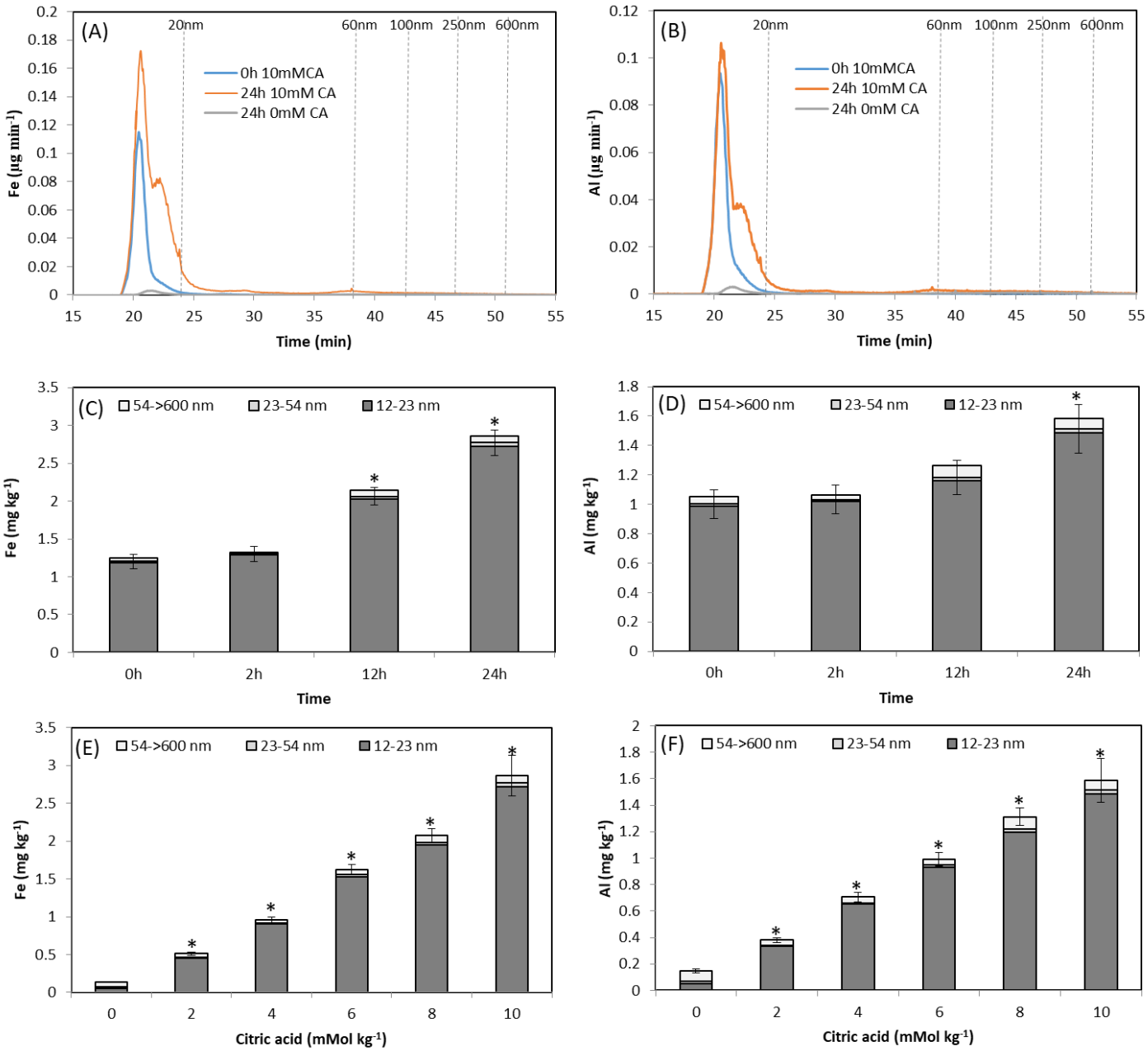

Figure 2. Iron (A) and aluminium (B) fractograms from asymmetric flow field-flow fractionation coupled to ICP-MS of water dispersed soil colloids before and after incubation with citric acid at increasing doses (filtered through 0.22 µm). Vertical dash lines mark the elution time of latex standards peaks (20, 60, 100, 250 and 600 nm). Integration of fractogram peaks for increasing incubation time (0, 2, 12 and 24) and citric acid dose of 10 mMol kg^{-1} soil for Iron(C) or aluminium (D). Integration of fractogram peaks for increasing citric acid dose (0, 2, 4, 6, 8, 10 mMol kg^{-1} soil) after 24 h of citric acid addition for Iron (E) or aluminium (F). Error bars represent standard deviation and * denote significant difference with respect to their respective controls (0 time or 0 dose, $P<0.05$, Tukey test).

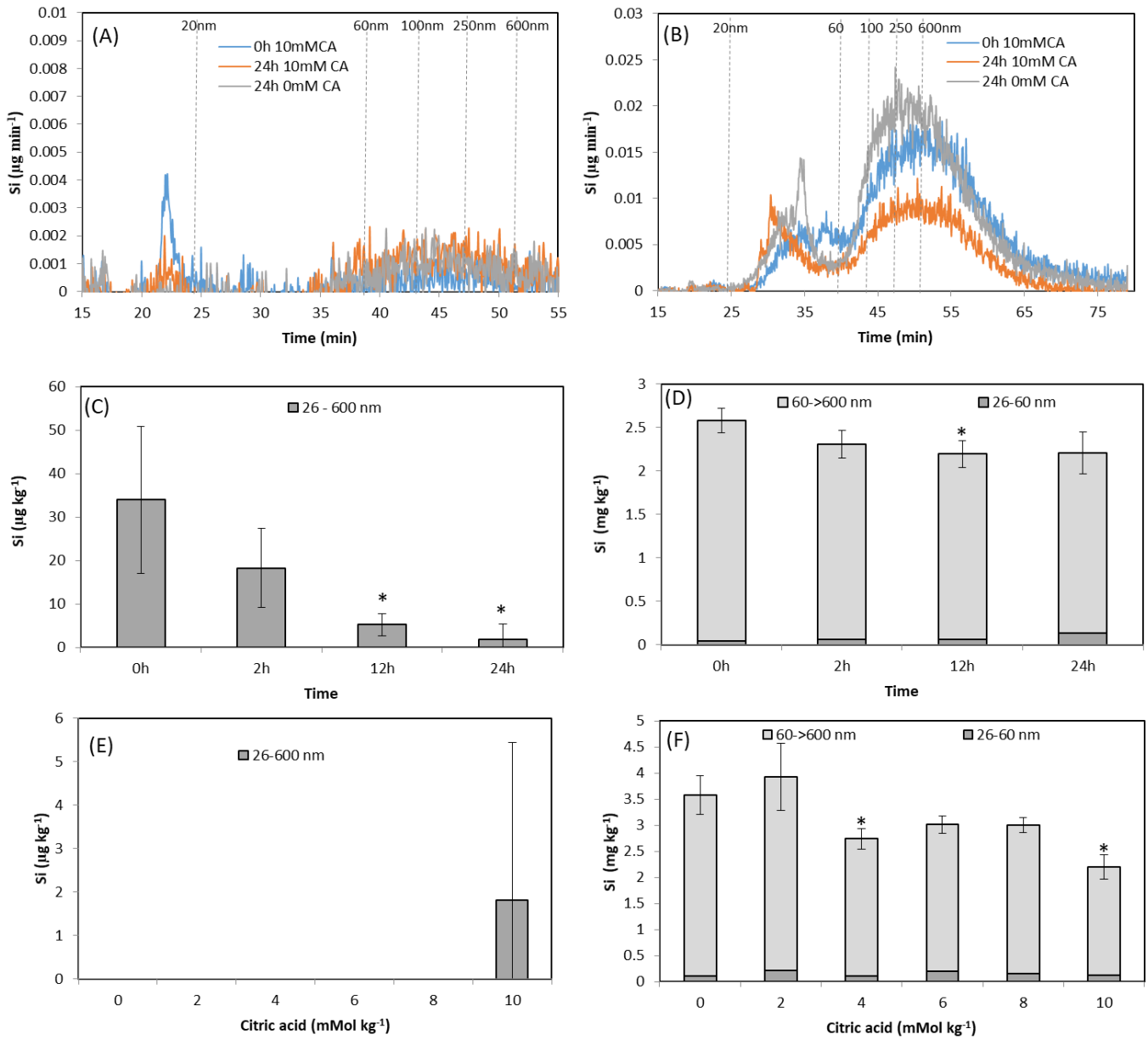

Figure 3. Silicon fractograms obtained by asymmetric flow field-flow fractionation coupled to ICP-MS for water dispersed soil colloids before and after incubation with citric acid at increasing doses [filtered through 0.22µm (A) or 5 µm (B)]. Vertical dash lines mark the elution time of from eluted latex standards peaks (20, 60, 100, 250 and 600 nm). Integration of fractogram peaks for increasing incubation time (0, 2, 12 and 24) and citric acid dose of 10 mMol kg^{-1} soil [filtered through 0.22µm (C) or 5 µm (D)]. Integration of fractogram peaks for increasing citric acid dose (0, 2, 4, 6, 8, 10 mMol kg^{-1} soil) after 24 h of citric acid addition [filtered through 0.22µm (E) or 5 µm (F)]. Error bars represent standard deviation and * denote significant difference with respect to their respective controls (0 time or 0 dose, $P<0.05$, Tukey test).

Table 1. General soil properties and phosphorus indices (Menezes-Blackburn et al. 2016b).

	Glensaugh soil
Olsen P (mg kg^{-1})	6.7
Calcium chloride P (mg kg^{-1})	0.08
Water P (mg kg^{-1}; 1:4 solid to liquid)	0.04
Water P (mg kg^{-1}; 1:10 solid to liquid)	0.19
Water P (mg kg^{-1}; 1:100 solid to liquid)	1.71
Aqua regia P (mg kg^{-1})	574
P saturation (oxalate)	10.5
Microbial P (mg kg^{-1})	0.49
C (%/w)	4.86
N (%/w)	0.43
C:N	11.37
pH (water)	5.1

Table 2. Total elemental concentrations (mg kg^{-1} soil dry weight) of the water extracts used for the asymmetric field-flow fractionation coupled to ICP-MS. Sample treatments (lines) correspond to eider the incubation of soil samples with 10 mMol kg^{-1} citric acid at increasing incubation time, or for a fixed incubation time (24h) with increasing citric acid dose. Samples were either syringe filtered through 0.22 or 5µm membranes. Values are followed by their standard error (SE) and an * indicate significant differences between the mean and its respective control (time 0 h or dose 0 mmol kg-1; Tukey, p<0.05).

	P		**P**		**C**		**C**		**Fe**		**Fe**		**Al**		**Al**		**Si**		**Si**	
	0.22 µm	**SE**	**5µm**	**SE**	**0.22 µm**	**SE**	**5µm**	**SE**	**0.22 µm**	**SE**	**5µm**	**SE**	**0.22 µm**	**SE**	**5µm**	**SE**	**0.22 µm**	**SE**	**5µm**	
Time (h)																				
0	2.4	0.4	2.2	0.3	454.6	83.3	553.9	120.1	57.0	14.5	50.3	12.0	76.2	18.8	81.5	19.5	7.2	1.8	50.3	12.0
2	2.2	0.3	2.2	0.2	435.0	80.8	796.9*	179.0	59.6	15.1	55.8	13.2	69.1	17.0	81.4	19.4	6.6	1.6	55.8	13.2
12	1.4*	0.1	2.3	0.3	419.7	70.5	685.7	151.7	63.1	16.0	54.8	12.5	65.8	16.1	83.7	19.4	7.3	1.7	54.8	12.5
24	0.9*	0.0	1.5*	0.1	339.9*	49.3	657.3	144.8	42.8*	10.9	50.4	11.9	48.5*	11.5	74.3	17.6	6.7	1.6	50.4	11.9
Dose (mmol kg^{-1})																				
0	0.4	0.0	0.6	0.0	173.7	16.4	354.2	64.2	0.6	0.1	2.8	0.0	1.1	0.2	5.7	0.4	5.0	1.2	2.8	0.0
2	0.5*	0.0	0.7*	0.1	203.2*	22.4	338.0	57.6	4.8*	1.2	4.4*	0.4	7.6*	1.7	9.5*	1.2	5.3	1.3	4.4*	0.4
4	0.5*	0.0	0.8*	0.0	203.2*	21.1	416.9	79.3	9.3*	2.4	10.6*	2.1	13.9*	3.2	21.7*	4.6	5.3	1.3	10.6*	2.1
6	0.6*	0.0	0.9*	0.0	271.5*	36.4	460.7*	89.0	19.9*	5.1	20.6*	4.5	25.4*	6.0	39.0*	8.8	5.8	1.4	20.6*	4.5
8	0.7*	0.0	1.0*	0.0	286.5*	38.5	560.2*	116.2	28.6*	7.3	29.9*	6.8	37.2*	8.8	51.8*	12.0	6.0	1.5	29.9*	6.8
10	0.9*	0.0	1.2*	0.0	339.9	49.3	561.2*	117.4	42.8*	10.9	41.9*	9.9	48.5*	11.5	61.6*	14.6	6.7*	1.6	41.9*	9.9

Table 3. Pearson correlation table between soil phosphorus bioavailability and desorption kinetics related parameters from Menezes Blackburn et al. (2016) (Menezes-Blackburn et al. 2016a) (columns) with the content of P, C, Fe, Al and Si in different size colloids separated by asymmetric field-flow fractionation coupled to ICP-MS. R values in bold indicate significant correlation at $p<0.05$.

	P_{OLSEN}	Pi_{DET}	Pi_{DGT}	PE	Desorpt.	Kdl	R	$R\text{-}R_{diff}$	Tc	K_1	K_{-1}
P (14-22 nm)	-0.61	**0.95**	**0.81**	**0.91**	**-0.83**	**-0.84**	**-0.79**	**-0.79**	**0.96**	**-0.73**	**-0.76**
P (22-34 nm)	-0.69	**0.84**	**0.80**	**0.75**	-0.69	-0.70	-0.62	-0.62	**0.86**	-0.52	-0.57
P (34-147 nm)	**-0.78**	**0.81**	**0.72**	0.68	-0.70	-0.66	-0.59	-0.59	**0.86**	-0.48	-0.54
P (14-147 nm)	-0.65	**0.94**	**0.82**	**0.89**	**-0.82**	**-0.83**	**-0.77**	**-0.77**	**0.96**	-0.69	**-0.73**
C (13-15 nm)	-0.53	**0.99**	0.70	**0.96**	**-0.95**	**-0.98**	**-0.96**	**-0.96**	**0.97**	**-0.92**	**-0.94**
C (15-24 nm)	-0.38	**0.96**	**0.72**	**0.99**	**-0.90**	**-0.98**	**-0.97**	**-0.97**	**0.90**	**-0.95**	**-0.94**
C (24-34 nm)	-0.34	**0.89**	**0.97**	**0.88**	-0.66	**-0.80**	-0.70	-0.70	**0.88**	-0.61	-0.62
C (34-100 nm)	-0.46	**0.99**	**0.81**	**0.98**	**-0.89**	**-0.96**	**-0.92**	**-0.92**	**0.96**	**-0.87**	**-0.88**
C (13-100 nm)	-0.41	**0.98**	**0.78**	**0.99**	**-0.89**	**-0.97**	**-0.94**	**-0.94**	**0.94**	**-0.91**	**-0.91**
Al (14-26 nm)	-0.33	**0.96**	**0.74**	**0.98**	**-0.89**	**-0.99**	**-0.96**	**-0.96**	**0.91**	**-0.94**	**-0.93**
Al (80- 1k nm)	0.37	**-0.76**	-0.42	**-0.85**	**0.80**	**0.78**	**0.83**	**0.83**	**-0.71**	**0.86**	**0.86**
Si (14-60 nm)	**-0.94**	0.40	0.15	0.16	-0.47	-0.21	-0.21	-0.21	0.53	-0.11	-0.22
Si (60- 1k nm)	0.34	**-0.78**	-0.48	**-0.88**	**0.80**	**0.80**	**0.84**	**0.84**	**-0.73**	**0.86**	**0.86**
Fe (14-25 nm)	-0.41	**0.98**	**0.77**	**0.99**	**-0.90**	**-0.98**	**-0.95**	**-0.95**	**0.93**	**-0.92**	**-0.92**
Fe (60 - 1k nm)	0.38	**-0.81**	-0.50	**-0.90**	**0.83**	**0.83**	**0.86**	**0.86**	**-0.76**	**0.88**	**0.88**

Bicarbonate extractable P (P_{OLSEN}); Soil solution inorganic P (P_{iDET}); DGT measured bioavailable inorganic P (P_{iDGT}); Effective inorganic P supply accounting to both diffusion and desorption processes (P_E); P desorption rate (Desorpt.); Ratio between sorbed and soil solution P (Kdl); Ratio between P_{iDET} and P_{iDGT} (R); P supplied by desorption relative to soil solution P initial concentration (R-Rdiff); Soil solution equilibration time (Tc); P adsorption rate constant (K_1); P desorption rate constant (K_{-1}).

632 **Supplementary material**

633 **Table S1** Soil phosphorus desorption parameters from Menezes-Blackburn et al. (2016) [1]

634

Dose	pH	POlsen (mg/kg)	Pi-DET (mg/L)	Pi-DGT (µg/l)	PE (µg/kg)	Desorpt (mg/L/day)	Kdl (cm^3 /g)	R	R-R-diff	Tc (s)	K1 (1/s)	K-1 (1/s)
0	5.2	9.524	0.03	6.4	0.12	0.085	292	0.196	0.141	1.329	2.1E-04	4.2E-07
2	5.1	10.480	0.04	8.0	0.13	0.108	265	0.202	0.148	1.235	2.2E-04	4.9E-07
4	4.9	10.373	0.05	6.8	0.13	0.079	219	0.145	0.090	2.711	1.0E-04	2.7E-07
6	4.8	10.163	0.07	7.3	0.14	0.063	144	0.103	0.049	7.264	3.8E-05	1.5E-07
8	4.7	9.608	0.11	7.8	0.15	0.035	88	0.072	0.017	23.458	1.2E-05	7.8E-08
10	4.7	9.516	0.13	9.1	0.17	0.036	73	0.069	0.015	28.667	9.7E-06	7.7E-08

635

636 **Table S2.** Carbon to phosphorus (C:P) and aluminium to iron (Al:Fe) of different eluted colloids during
637 the asymmetric flow field-flow fractionation coupled to ICP-MS analysis of fine water dispersed soil
638 colloids before and after incubation with citric acid at increasing doses or increasing incubation time (0,
639 2, 12 and 24h) and citric acid dose of 10 mMol kg^{-1} soil (filtered through 0.22µm)

	C:P				**Al:Fe**	
Incubation Time	**Peak 1**	**Peak 2**	**Peak 3**	**all**	**Peak 1**	**All**
0h	70.7	345.1	377.4	155.6	0.8	0.8
2h	74.7	338.5	372.7	149.9	0.8	0.8
12h	101.7	416.7	448.2	197.5	0.6	0.6
24h	112.8	385.8	424.6	206.8	0.5	0.6
Dose of citric acid	**Peak 1**	**Peak 2**	**Peak 3**	**all**	**Peak 1**	**All**
0	103.7	390.3	411.1	215.4	1.0	1.1
2	110.8	416.9	434.5	227.7	0.7	0.7
4	121.8	437.7	489.7	239.2	0.7	0.7
6	134.4	403.7	450.1	241.1	0.6	0.6
8	120.3	400.3	435.3	222.3	0.6	0.6
10	112.8	385.8	424.6	206.8	0.5	0.6

640

641

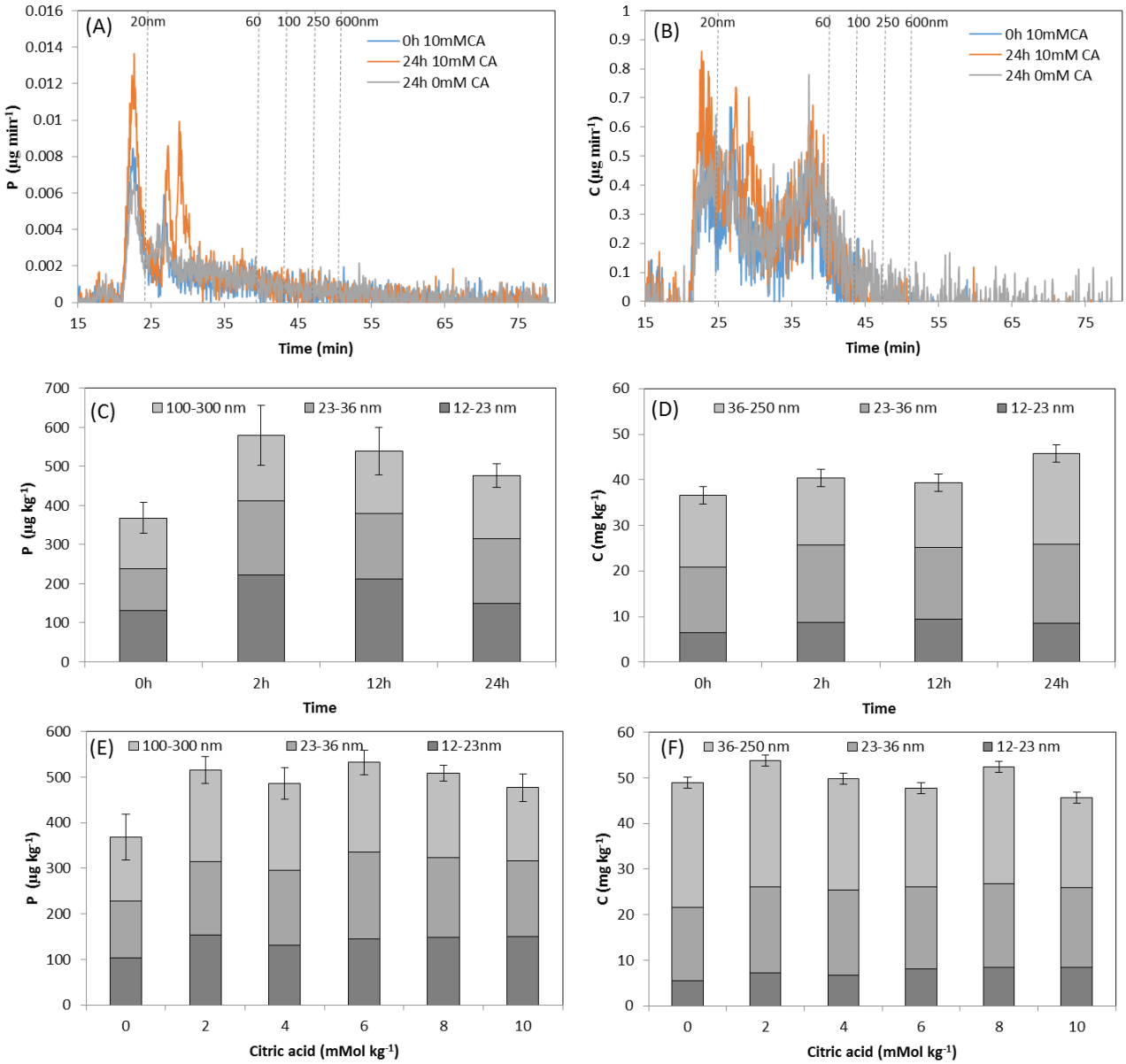

Figure S1. Phosphorus (A) and Carbon (B) fractograms from asymmetric flow field-flow fractionation coupled to ICP-MS analysis of water dispersed soil colloids before and after incubation with citric acid at increasing doses (filtered through 5µm). Vertical dash lines mark the elution time of from eluted latex standards peaks (20, 60, 100, 250 and 200 nm). Integration of fractogram peaks for increasing incubation time (0, 2, 12 and 24) and citric acid dose of 10 mMol kg^{-1} soil for phosphorus (C) or Carbon (D). Integration of fractogram peaks for increasing citric acid dose (0, 2, 4, 6, 8, 10 mMol kg^{-1} soil) after 24 h of citric acid addition for phosphorus (E) or Carbon (F)

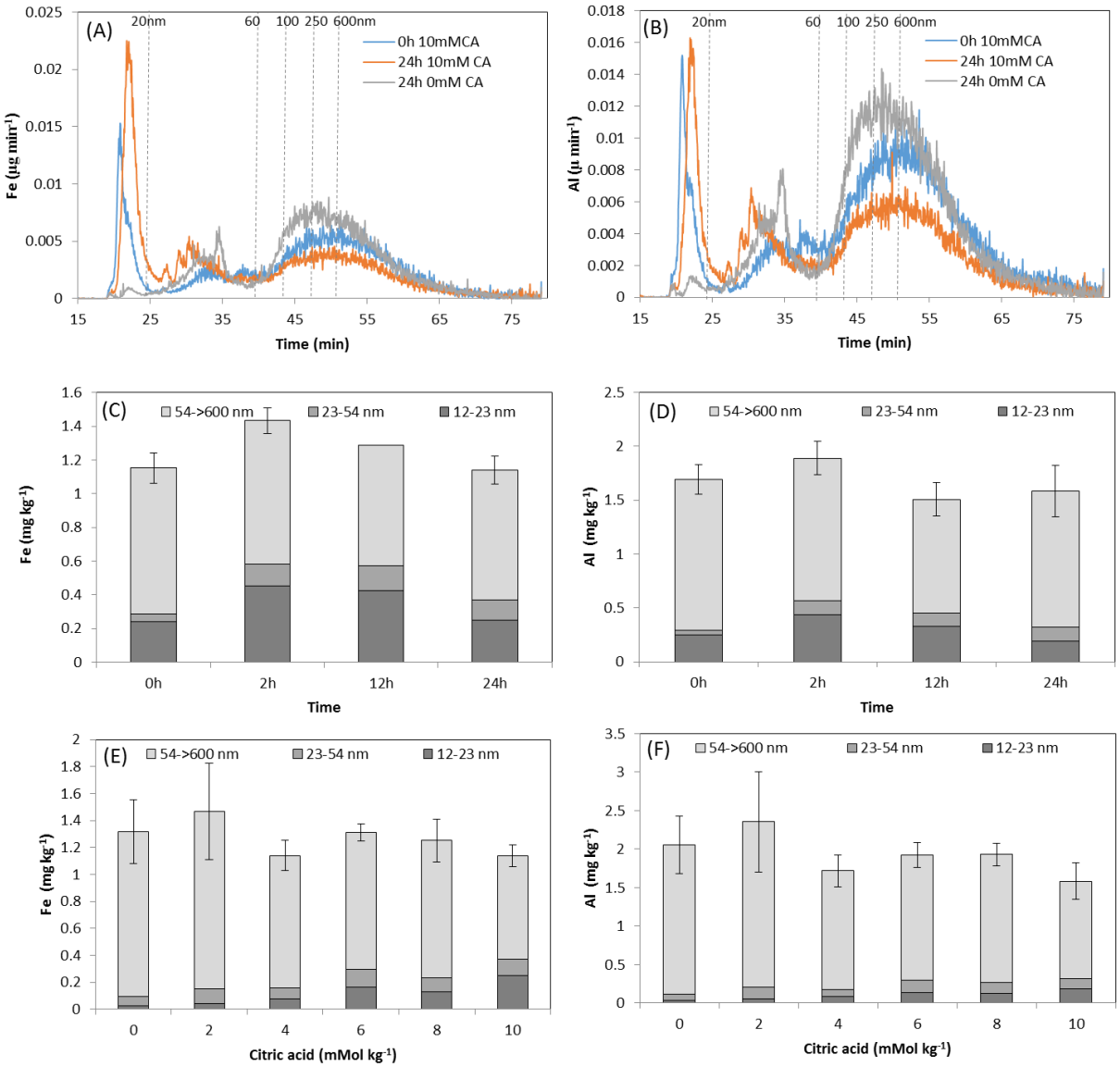

Figure S2. Iron (A) and Aluminium (B) fractograms from asymmetric flow field-flow fractionation coupled to ICP-MS analysis of water dispersed soil colloids before and after incubation with citric acid at increasing doses (filtered through 5µm). Vertical dash lines mark the elution time of from eluted latex standards peaks (20, 60, 100, 250 and 200 nm). Integration of fractogram peaks for increasing incubation time (0, 2, 12 and 24h) and citric acid dose of 10 mMol kg^{-1} soil for Iron(C) or Aluminium (D). Integration of fractogram peaks for increasing citric acid dose (0, 2, 4, 6, 8, 10 mMol kg^{-1} soil) after 24 h of citric acid addition for Iron (E) or Aluminium (F).